Journal of Applied Electrochemistry (2006) 36:567–576
DOI 10.1007/s10800-005-9107-6

A model for the electrochemical reduction of 2-ethylpicolinate under galvanostatic control

A.M. ROMULUS*, J. LOZAR and A. SAVALL
*Laboratoire de Génie Chimique, UMR CNRS 5503, Université Paul Sabatier, 31062, Toulouse Cedex 9, France (*author for correspondence, tel.: +33-0-561558677, fax: +33-0-561556139, e-mail: romulus@chimie.ups-tlse.fr)*

Received 17 March 2005; accepted in revised form 2 December 2005

Key words: 2-ethylpicolinate, 2-hydroxymethylpyridine, electrochemical reduction, galvanostatic control, modelling

Abstract

A model is presented for the variation in reactant concentrations during the electrochemical reduction of 2-ethylpicolinate on a lead cathod in sulphuric acid solutions under galvanostatic conditions. The electrolyses were performed in a laboratory filter-press reactor. Successive or parallel electrochemical reactions coupled with chemical reactions are taken into account, according to a reaction scheme in agreement with the experimental results. Analytical expressions are used to describe the progress of the various reactions, taking into account both chemical and electrochemical kinetics and transfer properties. All reactions are assumed to be first or pseudo-first order. The variations in charge-transfer rate constants are considered as functions of reactant conversion. The effects of acidity, current efficiency, initial concentration of 2-ethylpicolinate and temperature are presented. The model aims at estimating the yield of electrolysis products under the experimental conditions necessary for obtaining 2-hydroxymethylpyridine in optimum quantities.

Symbols

C_X	concentration of species **X** in the cathodic compartment (mol m^{-3})
C^0_X	initial concentration of species **X** in the cathodic compartment (mol m^{-3})
C_{XS}	concentration of species **X** at the surface of electrode (mol m^{-3})
c	width of cathodic compartment (direction perpendicular to flow) (31×10^{-3} m)
D_X	diffusion coefficient of species **X** (m^2 s^{-1})
$d_h = \frac{2ch}{c+h}$	equivalent hydraulic diameter (5.47×10^{-3} m)
$E(t)$	electrode potential at t/ECS (V)
$E_i(I=0)$	electrode potential/ECS (V), at $I=0$ for the electrochemical reaction i
$F=96487$	Faraday's constant (C mol^{-1})
h	thickness of the cathodic compartment (direction perpendicular to flow) (3×10^{-3} m)
$[H_2SO_4]$	sulphuric acid concentration (mol dm^{-3} in the formulas)
I	electrolysis current (A)
j	electrolysis current density (A m^{-2})
j_i	current density of the electrochemical reaction i (A m^{-2})
k_{dX}	mass-transfer coefficient of species **X** (m s^{-1})
k_{fi}	charge-transfer constant for the electrochemical reaction i (m s^{-1})
k_{fi0}	charge transfer constant without overvoltage for the electrochemical reaction i (m s^{-1})
k_i	rate constant for the chemical reaction i
k'_i	apparent rate constant for the chemical reaction i
M_X	molar mass of species **X** (g mol^{-1})
n	number of electrons exchanged
p	parameter for the expression of R_f
Q	charge at time t per mol of reactant (F mol^{-1})
Q_V	flow rate (12.8×10^{-6} m^3 s^{-1})
r_i	rate of the chemical reaction i
$R=8.314$	ideal gas constant (J K^{-1} mol^{-1})
$Re = \frac{Q_V d_h}{\Omega_V}$	Reynolds number
R_f	faradaic yield
R_X	chemical yield in species **X**
s	slope

S	area of cathode (14×10^{-4} m^2)
$Sc=\frac{v}{D_X}$	Schmidt number
T	absolute temperature (K)
V_{mX}	molar volume of species **X** in solution at boiling point (m^3 kmol^{-1})
V_S	volume of catholyte (0.15×10^{-3} m^3)
Y_i ($i=1$ to 11)	coefficient (m s^{-1})
Z_i ($i=2$, 3, 4, 6)	ratio between different charge-transfer pairs
α_i	charge transfer coefficient for the electrochemical process i
θ	temperature (°C)
μ	dynamic viscosity of solution assumed to be equivalent to a sulphuric acid solution (N s m^{-2})
$v=\frac{\mu}{\rho}$	kinematic viscosity of the solution (m^2 s^{-1})
ρ	voluminal mass of solution (kg m^{-3})
$\Omega=ch$	cross-section area of the cathodic compartment (93×10^{-6} m^2)

1. Introduction

During a preparative electrolysis, the variation in reactant concentration depends on mass-transfer conditions in the reactor and charge-transfer constants. In this work electrolyses were performed under galvanostatic control. Modelling of this type of electrolysis is difficult because the variation in time of the electrode potential is correlated with the variations in charge-transfer rate constants for the electroactive species. So the products can be strikingly different from those obtained with potentiostatic control.

The theoretical analysis of galvanostatic electrolysis, with or without recycling, involving electrochemical and chemical reactions in series and in parallel, has already been presented to predict the variation with time of the concentrations of reactants or their spatial distribution in the reactor [1–10]. Similar studies have been performed for electrolyses with potentiostatic control, to predict variations in space and time [11–17].

In this paper the model uses experimental results for the electroreduction of 2-ethylpicolinate to prepare 2-hydroxymethylpyridine [18]. This compound is a heterocyclic alcohol used as intermediate for the synthesis of pharmaceutical and agrochemical products, while 2-ethylpicolinate is an available raw material. In acidic aqueous solutions this ester can be partially hydrolysed into picolinic acid, which is less reducible. Experimental results and literature analysis show that these reductions involve complex processes. Successive reductions of ester and carboxylic acid are coupled firstly with reductions of the pyridinic nucleus and/or the solvent and secondly with ester hydrolysis or aldehyde hydrate dehydration [19–20]. To produce the 2-hydroxymethylpyridine a lead cathode and a sulphuric acid medium were selected, so that the reductions of the ester function or of the carboxylic acid function prevail over of those of the pyridinic nucleus [18–19, 21].

This work presents numerical modelling of the variation in reactant concentration during electrolysis. The successive and parallel electrochemical or chemical reactions, which concern the ester or carboxylic acid or pyridinic functions, are taken into account in the mathematical analysis. The solvent reduction is estimated by analysing the experimental faradaic yield. Analysis of the experimental data allows the charge-transfer rate constants of the electroactive species to be determined.

2. Experimental details

The electrolyses of aqueous sulphuric acid solutions of 2-ethylpicolinate were carried out on a lead cathode under galvanostatic control. These solutions contain various quantities of picolinic acid resulting from the spontaneous hydrolysis of 2-ethylpicolinate. The filter press reactor (ELECTROCELL AB, Sweden) had two compartments separated by a cationic membrane (NAFION 423, Dupont de Nemours, USA). The volumes of catholyte and anolyte were both 150 cm^3. The electrolyte flow rate in each loop was 12.8 cm^3 s^{-1}. The cathodic cell compartment contained a lead sheet with a surface area of 14 cm^2. The pyridine derivatives were assayed by liquid-phase chromatography (HPLC) during electrolysis. All the experimental details have been described previously [18–20]. Table 1 shows several operating conditions for the electrolyses performed: initial reactant concentrations, temperature, current density, sulphuric acid concentration and total electric charge.

3. Calculation

3.1. *Reaction scheme*

The chemical formulas of the different species used in developing the model are given, with just an example for **(E)** and **(E′)**:

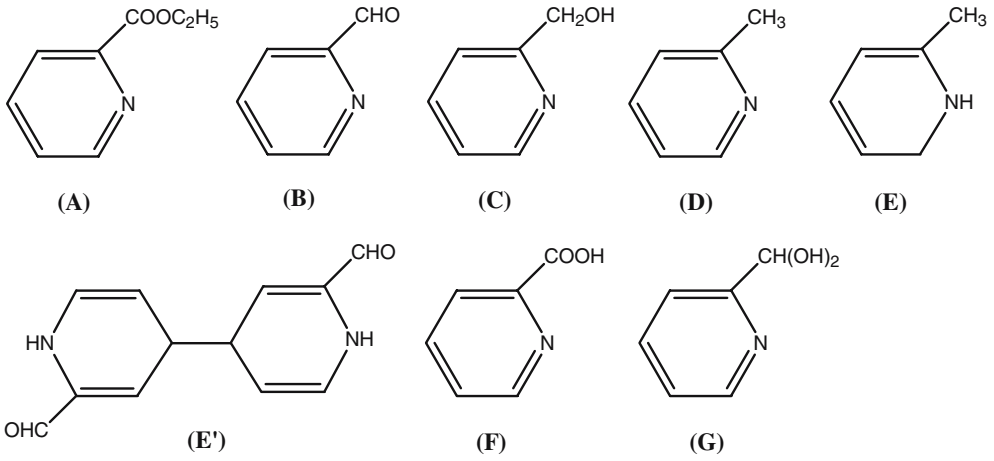

The electrochemical reduction of 2-ethylpicolinate **A** takes place preferentially on the ester function under the experimental conditions selected [19]. The reaction leads to 2-formylpyridine **B**, which is reduced to 2-hydroxymethylpyridine **C** then to picoline **D**, as follows (Pyr represents the pyridine nucleus):

$$\mathrm{PyrCOOC_2H_5(\mathbf{A}) + 2e + 2H^+ \rightarrow PyrCHO\ (\mathbf{B}) + C_2H_5OH} \quad (1)$$

$$\mathrm{PyrCHO\ (\mathbf{B}) + 2e + 2H^+ \rightarrow PyrCH_2OH\ (\mathbf{C})} \quad (2)$$

$$\mathrm{PyrCH_2OH\ (\mathbf{C}) + 2e + 2H^+ \rightarrow PyrCH_3(\mathbf{D}) + H_2O} \quad (3)$$

In parallel with the reduction of the side chain, electrohydrogenation of the **B** and **D** nucleus may occur [18–19]. In these earlier papers, competing reductions were detected by HPLC, showing a decrease in the mass balance related to the pyridinic derivatives. The products of electrohydrogenation are generally present in small amounts as long as the maximum quantity of **B** is not reached or as long as **D** is not significantly formed (i.e. $>2\%$ of the initial 2-ethylpicolinate concentration). Electrohydrogenation of the pyridinic nucleus is generally coupled with the production of polymers [22–24]. In this work the electrolyses were stopped before complete electrohydrogenation of the pyridinic nucleus, the main experimental objective being the identification of optimum conditions for obtaining the maximum amount of **C**. Reductions of the aromatic nucleus in **B** and **D** lead to the production of dihydropicoline **E** and dimer **E′** [22–23], as follows:

$$\mathrm{PyrCH_3(\mathbf{D}) + 2e + 2H^+ \rightarrow C_6H_9N\ (\mathbf{E})} \quad (4a)$$

$$\mathrm{PyrCHO\ (\mathbf{B}) + e + H^+ \rightarrow 1/2\ C_{12}H_{12}N_2O_2(\mathbf{E'})} \quad (4b)$$

The experimental results show that the molar balance decrease occurs mainly after the production of **D**: therefore only reduction (4a) is taken into account [18]. In parallel with these reductions, **A** is hydrolysed into picolinic acid **F** in aqueous sulphuric acid medium:

$$\mathrm{PyrCOOC_2H_5(\mathbf{A}) + H_2O \rightarrow PyrCOOH\ (\mathbf{F}) + C_2H_5OH} \quad (5)$$

The carboxylic group of picolinic acid can be reduced under the previous experimental conditions [19]. This reduction leads to the hydrate **G**, which is a

Table 1. Experimental conditions for various electrolyses

Experiment	C_A^0/mol m^{-3}	C_F^0/mol m^{-3}	θ/°C	j/A m^{-2}	[H_2SO_4]/mol dm^{-3}	$Q_{max.}$/F mol^{-1}
1	215	33	50	1071	3	6.06
2	235	11	50	1071	5	4.35
3	235	11	50	1071	7	4.97
4	212	22	50	1071	9	9.07
5	228	17	50	571	3	6.96
6	215	31	50	571	5	3.70
7	203	42	50	571	7	4.90
8	988	0	50	1071	5	2.92
9	220	18	20	1071	3	5.21

C_A^0, C_F^0: 2-ethylpicolinate **A** and picolinic acid **F** initial concentrations; θ: temperature; j: total current density; [H_2SO_4]: sulphuric acid molarity; Q_{max}: total electric charge through the reactor.

non-reducible intermediate product [21, 25]. The dehydration of **G** leads to **B**. The reactions are as follows:

$$\mathrm{PyrCOOH}(\mathbf{F}) + 2\mathrm{e} + 2\mathrm{H}^+ \rightarrow \mathrm{PyrCH(OH)_2}(\mathbf{G}) \quad (6)$$

$$\mathrm{PyrCH(OH)_2}(\mathbf{G}) \rightarrow \mathrm{PyrCHO}(\mathbf{B}) + \mathrm{H_2O} \quad (7)$$

Hydrogen evolution is catalysed by the pyridinic derivatives [23–26]. The reaction scheme involves the reduction of the solvent, which is detected by a decrease in faradaic yield at the end of electrolysis. At any time during electrolysis, the faradaic yield is defined as the ratio of the electric charge used for the reductions (1), (2), (3), (4a) and (6) to the total electric charge used for the electrolysis at that time.

Finally, the reaction scheme for the reduction of 2-ethylpicolinate **A** is as follows:

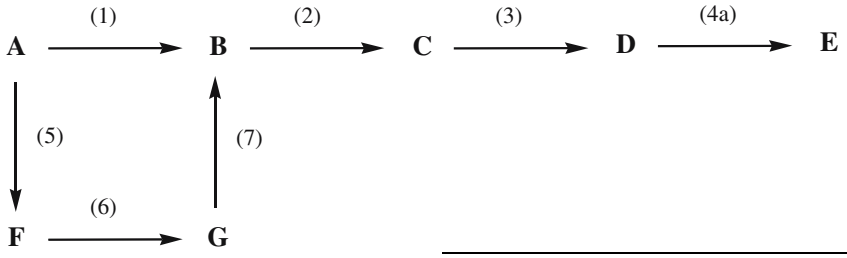

3.2. *Mathematical development*

All electrochemical and chemical reactions taken into account are as follows:

(1) $\mathbf{A} + 2e + 2\mathrm{H}^+ \rightarrow \mathbf{B} + \mathrm{C_2H_5OH} \quad (j_1, k_{\mathrm{f}1})$
(2) $\mathbf{B} + 2e + 2\mathrm{H}^+ \rightarrow \mathbf{C} \quad (j_2, k_{\mathrm{f}2})$
(3) $\mathbf{C} + 2e + 2\mathrm{H}^+ \rightarrow \mathbf{D} + \mathrm{H_2O} \quad (j_3, k_{\mathrm{f}3})$
(4a) $\mathbf{D} + 2e + 2\mathrm{H}^+ \rightarrow \mathbf{E} \quad (j_4, k_{f4})$
(5) $\mathbf{A} + \mathrm{H_2O} \rightarrow \mathbf{F} + \mathrm{C_2H_5OH} \quad (k_5)$
(6) $\mathbf{F} + 2e + 2\mathrm{H}^+ \rightarrow \mathbf{G} \quad (j_6, k_{\mathrm{f}6})$
(7) $\mathbf{G} \rightarrow \mathbf{B} + \mathrm{H_2O} \quad (k_7)$

The electron exchanges in the reaction scheme are described using the charge-transfer kinetic equations of the reducible species at the cathode. These equations use the charge-transfer rate constants $k_{\mathrm{f}}i$ of the various reductions. Mass transfer near the cathode is taken into account through the mass-transfer coefficient for each species k_{dX} in the filter press reactor. The charge-transfer and mass-transfer equations lead to a set of relationships between the current density j_i expressed for each reduction and the bulk concentration of each reducible derivative C_{X}. The formation rate for each species is expressed according to a first or pseudo-first order law, both for the chemical and the electrochemical reactions.

The charge-transfer equations are given in Equations (8) to (12):

$$\frac{j_1}{2F} = k_{\mathrm{f}1} C_{\mathrm{AS}} \quad (8)$$

$$\frac{j_2}{2F} = k_{\mathrm{f}2} C_{\mathrm{BS}} \quad (9)$$

$$\frac{j_3}{2F} = k_{\mathrm{f}3} C_{\mathrm{CS}} \quad (10)$$

$$\frac{j_4}{2F} = k_{\mathrm{f}4} C_{\mathrm{DS}} \quad (11)$$

$$\frac{j_6}{2F} = k_{\mathrm{f}6} C_{\mathrm{FS}} \quad (12)$$

The mass-transfer equations are given in Equations (13) to (17):

$$\frac{j_1}{2F} = k_{\mathrm{dA}}(C_{\mathrm{A}} - C_{\mathrm{AS}}) \quad (13)$$

$$\frac{j_2 - j_1}{2F} = k_{\mathrm{dB}}(C_{\mathrm{B}} - C_{\mathrm{BS}}) \quad (14)$$

$$\frac{j_3 - j_2}{2F} = k_{\mathrm{dC}}(C_{\mathrm{C}} - C_{\mathrm{CS}}) \quad (15)$$

$$\frac{j_4 - j_3}{2F} = k_{\mathrm{dD}}(C_{\mathrm{D}} - C_{\mathrm{DS}}) \quad (16)$$

$$\frac{j_6}{2F} = k_{\mathrm{dF}}(C_{\mathrm{F}} - C_{\mathrm{FS}}) \quad (17)$$

Equations (18) to (22) relating the current densities and the concentrations of the different species in the reactor are obtained by eliminating surface concentrations between the two sets of Equations (8) to (12) and (13) to (17):

$$\frac{j_1}{2F} = Y_1 C_{\mathrm{A}} \quad (18)$$

$$\frac{j_2}{2F} = Y_2 C_{\mathrm{A}} + Y_3 C_{\mathrm{B}} \quad (19)$$

$$\frac{j_3}{2F} = Y_4 C_{\mathrm{A}} + Y_5 C_{\mathrm{B}} + Y_6 C_{\mathrm{C}} \quad (20)$$

$$\frac{j_4}{2F} = Y_7 C_{\mathrm{A}} + Y_8 C_{\mathrm{B}} + Y_9 C_{\mathrm{C}} + Y_{10} C_{\mathrm{D}} \quad (21)$$

$$\frac{j_6}{2F} = Y_{11}C_F \tag{22}$$

The expressions for the coefficients Y_i, which depend upon charge-transfer constants k_fi and mass-transfer coefficients k_{dX}, are given in Appendix 1.

The rate of formation of each species is expressed in Equations (23) to (29), where the chemical rates of the reactions (5) and (7) are taken into account:

$$\frac{dC_A}{dt} = -\frac{S}{V_S}\frac{j_1}{2F} - k_5C_A \tag{23}$$

$$\frac{dC_B}{dt} = -\frac{S}{V_S}\frac{j_2 - j_1}{2F} + k_7C_G \tag{24}$$

$$\frac{dC_C}{dt} = \frac{S}{V_S}\frac{j_2 - j_3}{2F} \tag{25}$$

$$\frac{dC_D}{dt} = \frac{S}{V_S}\frac{j_3 - j_4}{2F} \tag{26}$$

$$\frac{dC_E}{dt} = \frac{S}{V_S}\frac{j_4}{2F} \tag{27}$$

$$\frac{dC_F}{dt} = -\frac{S}{V_S}\frac{j_6}{2F} + k_5C_A \tag{28}$$

$$\frac{dC_G}{dt} = \frac{S}{V_S}\frac{j_6}{2F} - k_7C_G \tag{29}$$

Finally, when the current densities are replaced by the expressions in Equations (18) to (22), the final set of Equations (30) to (36) is obtained that describes the time variations of the concentrations of the different species:

$$\frac{dC_A}{dt} = -\left(\frac{S}{V_S}Y_1 + k_5\right)C_A \tag{30}$$

$$\frac{dC_B}{dt} = -\frac{S}{V_S}[(Y_2 - Y_1)C_A + Y_3C_B] + k_7C_G \tag{31}$$

$$\frac{dC_C}{dt} = \frac{S}{V_S}[(Y_2 - Y_4)C_A + (Y_3 - Y_5)C_B - Y_6C_C] \tag{32}$$

$$\frac{dC_D}{dt} = \frac{S}{V_S}[(Y_4 - Y_7)C_A + (Y_5 - Y_8)C_B + (Y_6 - Y_9)C_C - Y_{10}C_D) \tag{33}$$

$$\frac{dC_E}{dt} = \frac{S}{V_S}(Y_7C_A + Y_8C_B + Y_9C_C + Y_{10}C_D) \tag{34}$$

$$\frac{dC_F}{dt} = -\frac{S}{V_S}Y_{11}C_F + k_5C_A \tag{35}$$

$$\frac{dC_G}{dt} = \frac{S}{V_S}Y_{11}C_F - k_7C_G \tag{36}$$

Faradaic yield is the ratio between the theoretical electric charge necessary to produce the different reduction products and the electric charge received by the reactor. An experimental average faradaic yield between two successive measurements can be calculated from the differences in product concentration ΔC_X during the corresponding time interval Δt according to the formula:

$$R_f(t) = \frac{FV_S[2(\Delta C_B + \Delta C_G) + 4\Delta C_C + 6\Delta C_D + 8\Delta C_E]}{jS\Delta t} \tag{37}$$

The current density for proton reduction is given by the expression $j(1 - R_f(t))$, according to the following reaction:

$$2H^+ + 2e \rightarrow H_2 \tag{38}$$

Furthermore, the value of j during the galvanostatic electrolysis is given by the following sum:

$$j = j_1 + j_2 + j_3 + j_4 + j_6 + j(1 - R_f(t)) \tag{39}$$

i.e:

$$R_f(t)j = 2F[(Y_1 + Y_2 + Y_4 + Y_7)C_A + (Y_3 + Y_5 + Y_8)C_B + (Y_6 + Y_9)C_C + Y_{10}C_D + Y_{11}C_F] \tag{40}$$

In the galvanostatic mode, the charge-transfer constants can vary during the electrolyses so the coefficients Y_i, which depend on the charge-transfer constants, also vary. Calculations were performed assuming a constant ratio $Z_i (i = 2, 3, 4, 6)$ between the different couples of charge transfer constants during electrolysis:

$$k_{f2} = Z_2k_{f1} \tag{41}$$

$$k_{f3} = Z_3k_{f1} \tag{42}$$

$$k_{f4} = Z_4k_{f1} \tag{43}$$

$$k_{f6} = Z_6k_{f1} \tag{44}$$

This hypothesis makes it possible to have a single unknown k_{f1} in Equation (40). The expression for the charge-transfer constant k_fi can be taken as $k_{fi} = k_{bi0}\exp(-b_iE)$ with $k_{bi0} = k_{fi0}\exp(b_iE_{i(I=0)})$ and $b_i = \frac{\alpha_i n_i F}{RT}$, so $Z_i = \frac{k_{bi0}}{k_{b10}}\exp[-(b_i - b_0)E]$. Assuming that the Z_i factors are nearly constant implies that the b_i

coefficients are of the same order or the cathodic potential E is approximately constant during the electrolysis. This assumption is discussed in more detail in the following section.

The Equations (30) to (36) were solved numerically. The duration of each electrolysis was divided into time steps Δt. Each calculation began with a choice of values for Z_2, Z_3, Z_4 and Z_6. Once Equation (40) had been solved by Newton's method, the initial value of k_f1 could be calculated. The concentrations of reactants at time Δt were calculated by solving Equations (30) to (36), according to the method described in Appendix 2. This procedure was repeated until the end of electrolysis. Comparison with the experimental concentrations of reactants was made by calculating the sum of the squares of the differences between calculated and experimental concentrations. The minimum of this sum was determined using the SIMPLEX method: it results from it a suitable set of parameters Z_2, Z_3, Z_4 and Z_6.

The electrochemical reduction of 2-ethylpicolinate is achieved in two phases. Initially, the only products that appear are 2-formylpyridine **B** and 2-hydroxymethylpyridine **C**. Picoline **D** appears in the second part of the electrolysis when the maximum quantity of **B** is reached [18–20]. For these conditions calculations were performed without taking into account **D** and **E** in the first stage of electrolysis: $C_D = C_E = 0,\ j_3 = j_4 = 0,\ k_{f3} = k_{f4} = 0,\ \ Y_i(i = 4 \text{ to } 10) = 0,\ Z_3 = Z_4 = 0$. Equations (33) and (34) were not taken into account in that part of the calculation. Once the calculated maximum concentration of **B** was reached, all equations were taken into account in subsequent steps of the calculation and parameters Z_2, Z_3, Z_4, Z_6 were deduced by fitting, as well as the values of various charge-transfer coefficients k_fi at any time.

4. Results and discussion

Operating conditions for the 9 experiments selected are shown in Table 1. At the beginning of the electrolysis, there is generally a small quantity of picolinic acid **F** coming from the hydrolysis of 2-ethylpicolinate (Reaction (5)). The electric charge Q passed through the electrochemical reactor for 1 mole of substrate is calculated from the following equation:

$$Q = \frac{jSt}{(C_A^0 + C_F^0)V_S} \tag{45}$$

Table 2. Rate constants for chemical reactions (5) and (7)

θ/°C	20	50
k'_5/mol^{-1} dm^3 s^{-1}	1.24×10^{-8}	3.03×10^{-6}
k_7/s^{-1}	$0.041 + 0.041$ [H_2SO_4]	$0.120 + 0.120$ [H_2SO_4]

Q is an interesting parameter that allows experiments to be compared under various conditions. Thus the value $Q = 4F$ mol^{-1} indicates the theoretical charge necessary for the complete conversion of ***A*** or ***F*** into ***C***. The total electric charge received by the reactor during an electrolysis Q_{max} is a measure of the electrolysis progress. Rate constants k_5 and k_7 of chemical reactions (5) and (7) were calculated according to indications given in Appendix 3, and the results are presented in Table 2. Calculated values for the mass-transfer constants k_{DX} (see Appendix 4) are shown in Table 3. These values depend on liquid composition and temperature, and are very close to each other, as far as the various aromatic compounds are concerned. Experimental values of average faradaic yield $R_f(t)$ obtained from Equation (37) can be represented by a relationship with a single parameter p:

$$R_f(t) = 1 - \exp(-\frac{p}{t^2}) \tag{46}$$

Figure 1 shows the variation of $R_f(t)$ with the charge Q for various concentrations of sulphuric acid. The faradaic yield is equal to 1 at the beginning of the electrolysis, then it decreases when the solvent is reduced. Figure 1 shows that decrease becomes greater as the acidity is raised. Various calculations have shown that $R_f(t)$ is a critical parameter in the model. For example, when the value of $R_f(t)$ is arbitrarily fixed at 1 – while the actual value is much lower – the calculation no longer converges.

Figure 2 shows an example of calculated and experimental values for the concentrations of the pyridinic derivatives. The average deviation between the experimental data and the computed values is 8 mol m^{-3} for this experiment. The fit is similar in the other cases. Experimental values of k_{f1} can be deduced from the variation of the logarithm of the concentration of **A** with time. The slope of the curve ln C_A as function as time is $s = -\frac{d\ln C_A}{dt} = \frac{k_{f1}k_{dA}}{k_{f1}+k_{dA}}\frac{S}{V_S} + k_5$, according to Equation (30), thus $k_{f1} = \left[\frac{S}{V_S}\left(\frac{1}{s-k_5}\right) - \frac{1}{k_{dA}}\right]^{-1}$. The experimental values of ln C_A have been fitted using a second order polynomial law, allowing further differentiation and calculation of

Table 3. Mass transfer coefficients of different species according to Carlsson's correlation [28]

θ/°C	[H_2SO_4]/mol dm^{-3}	$k_{dA} \times 10^4$/m s^{-1}	$k_{dB} \times 10^4$/m s^{-1}	$k_{dC} \times 10^4$/m s^{-1}	$k_{dD} \times 10^4$/m s^{-1}	$k_{dF} \times 10^4$/m s^{-1}
20	3	1.47	1.55	1.52	1.48	1.54
50	3	2.61	2.74	2.69	2.62	2.72
50	5	1.90	1.99	1.96	1.90	1.98
50	7	1.52	1.60	1.57	1.53	1.59
50	9	1.21	1.28	1.25	1.22	1.27

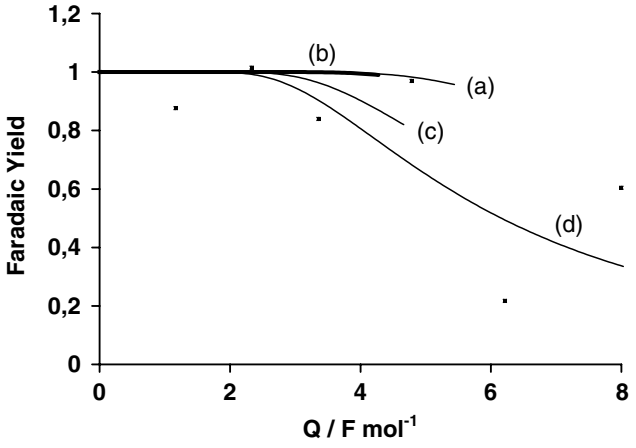

Fig. 1. Average faradaic yield for the electroreduction of 2-ethylpicolinate as a function of electric charge $Q(\theta = 50\,^{\circ}C$, $j = 1071$ A m^{-2}). Smoothed experimental results (Equation 37) in accordance with equation: $R_f(t) = 1 - \exp\frac{n}{t^2}$. Experimental data for curve (*d*) are represented. (a) $[H_2SO_4] = 3$ mol dm^{-3}; (b) $[H_2SO_4] = 5$ mol dm^{-3}; (c) $[H_2SO_4] = 7$ mol dm^{-3}; (d) $[H_2SO_4] = 9$ mol dm^{-3}.

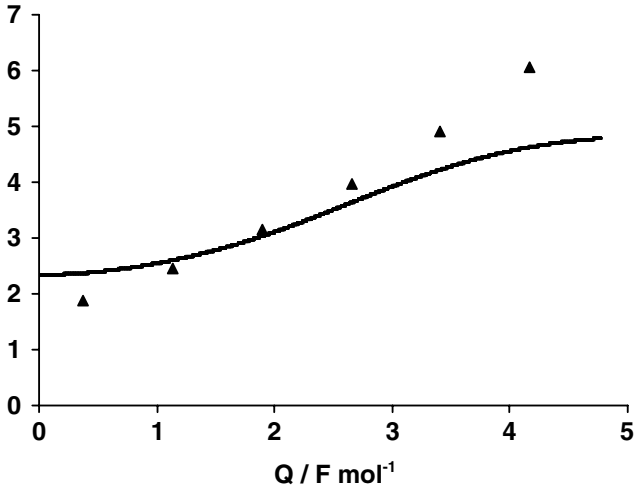

Fig. 3. Calculated (continuous curves) and experimental charge-transfer constant k_{f1}. Experiment 1: $C_A^0 = 215$ mol m^{-3}; $C_F^0 = 33$ mol m^{-3}; $j = 1071$ A m^{-2}; $[H_2SO_4] = 3$ mol l^{-1}; $\Theta = 50$ °C.

k_{f1}. Figure 3 shows the experimental and calculated values k_{f1}, which increase as the electrolysis progresses. The variation of k_{f1} reflects the time variation of overvoltage during electrolysis. The computed values vary by a factor less than 2 in the majority of cases, whereas the potential at the cathode is somewhat changed during the process, although in a reasonable manner. This assumption is validated by the fact that during the experiments, cathodic overvoltage remains constant until the beginning of the decrease in faradaic yield. As said before, picoline **D** appears in the calculation once the concentration of 2-formylpyridine **B** has reached a maximum. So the calculated curves of picoline and 2-hydroxymethylpyridine show a discontinuity. This results obviously from the change in the set of equations used in the calculation when the aldehyde has reached its maximum concentration. Finally, the good match between the experimental and calculated values of k_{f1} confirms the hypotheses adopted in the model. The calculated initial values of k_{f1} are reproducible when the initial conditions are identical. The initial value of k_{f1} is about 2.2×10^{-5} m s^{-1} for $j = 1071$ A m^{-2} and 1.2×10^{-5} m s^{-1} for $j = 571$ A m^{-2}. These results indicate that the initial potential of the cathode is the same from one experiment to another for the same current density value. When the concentration of substrate increases (experiment 8), the initial value of k_{f1} is logically lower.

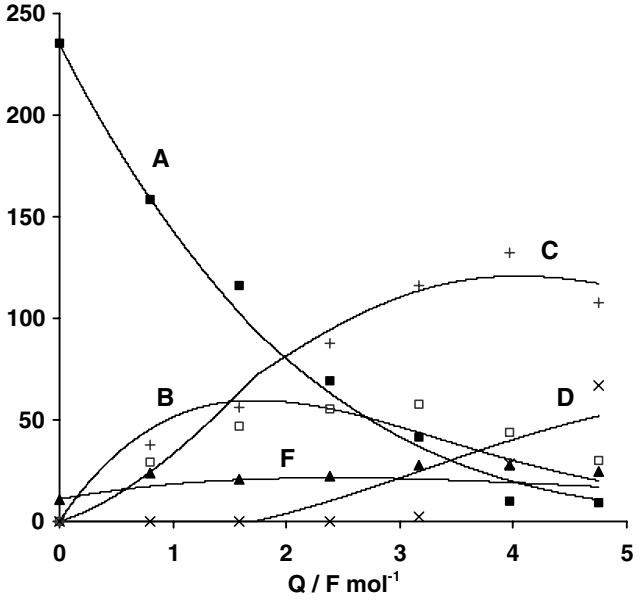

Fig. 2. Electrolysis of 2-ethylpicolinate **A**. Experiment 1: $C_A^0 = 215$ mol m^{-3}; $C_F^0 = 33$ mol m^{-3}; $j = 1071$ A m^{-2}; $[H_2SO_4] = 3$ mol l^{-1}; $\Theta = 50$ °C. Experimental data: **A** 2-ethylpicolinate **A**; **B** 2-formylpyridine; **C** 2-hydroxymethylpyridine; **D** picoline; **F** picolinic acid. Calculated concentrations: continuous curves.

Table 4 gives the values of the parameters Z_i corresponding to the best fit for each electrolysis. The interval of variation of the calculated value of the charge-transfer constant k_{f1} during an experiment is given in the last column. The values of Z_i parameters (successively Z_2 for 2-formylpyridine, Z_3 for 2-hydroxymethylpyridine, Z_4 for picoline and Z_6 for picolinic acid) characterize the ability for the reduction of the different species in relation to the reduction of the 2-ethylpicolinate **A** with respect to conditions of temperature, current density, acidity (see Table 1). Assumption that Z_i is constant during the process is somewhat restrictive but can be accepted with regard to the numerous parameters involved. This is in agreement with the assumptions of the calculation, i.e. the cathodic potential E is constant or the b_i are of the same order [20].

2-Formylpyridine is the most reducible compound, in accordance with the results indicated by the voltamperometric curves [18–20]: Z_2 values are greater than 1 and greater than the other Z_i values. However some Z_2 values are too low: in the first experiment, the value of 0.65 could mean that 2-formylpyridine is less reducible

Table 4. Ratios of charge-transfer constants

Experiment	$Z_2 = k_{f2}/k_{f1}$	$Z_3 = k_{f3}/k_{f1}$	$Z_4 = k_{f4}/k_{f1}$	$Z_6 = k_{f6}/k_{f1}$	$k_{f1} \times 10^5$/m s^{-1}
1	0.65	0.38	0.15	0.17	[2.6 – 10.4]
2	1.04	0.22	0.30	0.58	[2.3 – 6.7]
3	1.40	0.28	0.34	0.20	[2.0 – 6.5]
4	5.65	0.31	2.48	0.34	[2.0 – 3.1]
5	1.25	0.81	0.81	0.36	[1.2 – 1.7]
6	2.14	0.03	0	0.12	[1.3 – 3.4]
7	3.41	0	0	0.36	[1.2 – 2]
8	7.28	0.07	0.27	0.45	[0.5 – 1.2]
9	2.46	5.18	0.59	0.16	[1.5 – 2.2]

$Z_2 = k_{f2}/k_{f1}$; $Z_3 = k_{f3}/k_{f1}$; $Z_4 = k_{f4}/k_{f1}$; $Z_6 = k_{f6}/k_{f1}$. The last column indicates k_{f1} variation during electrolysis.

than 2-ethylpicolinate. This paradoxical result can be ascribed, in particular, to the difficulty in evaluating the faradaic yield $R_f(t)$. Indeed, the fact that only 5 concentration differences ΔC_X are used in obtaining $R_f(t)$ (Equation (37)) mathematically increases the numerical errors (see curve (*d*) of Figure 1).

Some other interesting correlations are obtained. The increase in acidity leads to the increase in Z_2 (compare experiments 1, 2, 3, 4 and on the other hand 5, 6, 7), according to the higher aldehyde reducibility with acidity. A decrease in current density gives the same result (compare experiments 1, 5; 2, 6 and 3, 7), in agreement with the experimental results of the voltamperometric curves [18–20].

At $j = 1071$ A m^{-2}, Z_3 values are not very sensitive to the variation in acidity. At $j = 571$ A m^{-2}, the values obtained are not completely reliable, probably because the electrolysis has not been taken far enough (see experiments 6 and 7). It should be noted that the value of $Z_3 = 0$ results from the absence of picoline **D**. The temperature increase leads to the decrease in Z_3 (compare experiments 1 and 9), improving the 2-hydroxymethypyridine yield.

The Z_4 value increases with acidity, going with the hydrogenation of picoline **D**. Otherwise, the values of parameters Z_4 and Z_6 are not easy to interpret with respect to the experimental results, probably because the amounts of **D**, **E** and **F** are very small.

Taking into account that the 2-hydroxymethylpyridine **C** is the valuable product of the reduction process, it is important to specify the optimum experimental conditions for obtaining a maximum yield in 2-hydroxymethylpyridine. A simulation of the electroreduction of **A** at 50 °C was performed with an initial concentration of 0.24 mol L^{-1} and with two different current densities 571 and 1071 A m^{-2}. The Z_i parameters were correlated with acidity using the values in Table 4. The computed maximum 2-hydroxymethylpyridine yield varies with the acidity. The calculation gives a maximum 2-hydroxymethylpyridine yield of 85% for sulphuric acid concentrations between 5 and 7 mol L^{-1}, with 571 A m^{-2} current density and 6 F mol^{-1} of electric charge received. This result can be compared with the maximum experimental yield found for the experimental conditions of Figure 4.

5. Conclusion

The products of reduction of 2-ethylpicolinate are, successively 2-formylpyridine, 2-hydroxymethylpyridine and picoline. Calculations were performed assuming that the ratios of the charge-transfer rate constants of the electroactive species remain constant during electrolysis. Solvent reduction, ester hydrolysis and picolinic acid reduction were also taken into account. The reliability of the model is based on the following main points. During electrolysis, the cathodic potential variation is small. Under these conditions, the calculation of the rate constant k_{f1} leads to small variations in rate constants with time. The calculation gives good agreement with experiments: the variation in concentration

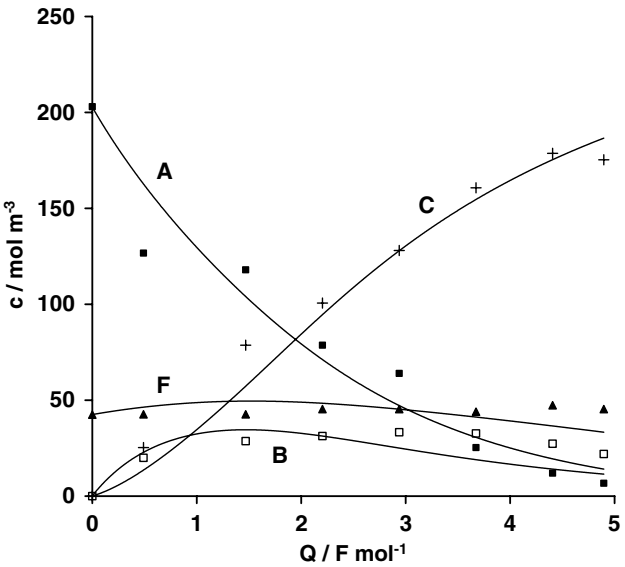

Fig. 4. Electrolysis of 2-ethylpicolinate **A**. Experiment 7: $C_A^0 = 203$ mol m^{-3}; $C_F^0 = 42$ mol m^{-3}; $j = 571$ A m^{-2}; $[H_2SO_4] = 3$ mol l^{-1}; $\Theta = 50$ °C. Experimental data: **A** 2-ethylpicolinate; **B** 2-formylpyridine; **C** 2-hydroxymethylpyridine; **F** picolinic acid. Calculated concentrations: continuous curves.

of the products depends on three main parameters: sulphuric acid concentration, current density and temperature. The yield of 2-hydroxymethylpyridine increases with acidity and temperature and decreases with current density. The best yield (85%) obtained using the model is in agreement with experiment.

Appendix 1: Expression for coefficients Y_i

$$Y_1 = \frac{k_{f1}k_{dA}}{k_{f1} + k_{dA}} \tag{47}$$

$$Y_2 = \frac{k_{f2}}{k_{f2} + k_{dB}} Y_1 \tag{48}$$

$$Y_3 = \frac{k_{f2}k_{dB}}{k_{f2} + k_{dB}} \tag{49}$$

$$Y_4 = \frac{k_{f3}}{k_{f3} + k_{dC}} Y_2 \tag{50}$$

$$Y_5 = \frac{k_{f3}}{k_{f3} + k_{dC}} Y_3 \tag{51}$$

$$Y_6 = \frac{k_{f3}k_{dC}}{k_{f3} + k_{dC}} \tag{52}$$

$$Y_7 = \frac{k_{f4}}{k_{f4} + k_{dD}} Y_4 \tag{53}$$

$$Y_8 = \frac{k_{f4}}{k_{f4} + k_{dD}} Y_5 \tag{54}$$

$$Y_9 = \frac{k_{f4}}{k_{f4} + k_{dD}} Y_6 \tag{55}$$

$$Y_{10} = \frac{k_{f4}k_{dD}}{k_{f4} + k_{dD}} \tag{56}$$

$$Y_{11} = \frac{k_{f6}k_{dF}}{k_{f6} + k_{dF}} \tag{57}$$

Appendix 2: Solution of Equations (30) to (36)

As an example Equation (30) is considered: $\frac{dC_A}{dt} = -(\frac{S}{V_S} Y_1 + k_5)C_A$, with $Y_1 = \frac{k_{f1}k}{k_{f1}+k_{dA}}$. The equation is integrated over a short time interval, which gives a calculation time step Δt. In this interval Y_1 is considered constant. Integration of the differential equation leads to a recurrence relationship relating concentrations C_A^i and C_A^{i-1} between moments t_{i-1} and $t_i = t_{i-1} + \Delta t$:

$$C_A^i = C_A^{i-1} - \left(\frac{S}{V_S} Y_1 + k_5\right) \int_{ti-1}^{ti} C_A dt \tag{58}$$

A trapezoidal integration gives:

$$C_A^i = C_A^{i-1} - \left(\frac{S}{V_S} Y_1 + k_5\right)(C_A^i + C_A^{i-1}) \frac{\Delta t}{2} \tag{59}$$

i.e.

$$C_A^i = C_A^{i-1} \frac{1 - (\frac{S}{V_S} Y_1 + k_5)\frac{\Delta t}{2}}{1 + (\frac{S}{V_S} Y_1 + k_5)\Delta t} \tag{60}$$

Similar calculations lead to relationships between C_X^i and C_X^{i-1}:

$$C_B^i = \frac{C_B^{i-1}(1 - \frac{SY_3\Delta t}{2V_S}) + \frac{S(Y_1 - Y_2)\Delta t}{2V_S}(C_A^i + C_A^{i-1}) + k_7(C_G^i + C_G^{i-1})\frac{\Delta t}{2}}{1 + \frac{SY_3\Delta t}{2V_S}} \tag{61}$$

$$C_C^i = \frac{C_C^{i-1}(1 - \frac{SY_6\Delta t}{2V_S}) + \frac{S(Y_2 - Y_4)\Delta t}{2V_S}(C_A^i + C_A^{i-1}) + \frac{S(Y_3 - Y_5)\Delta t}{2V_S}(C_B^i + C_B^{i-1})}{1 + \frac{SY_6\Delta t}{2V_S}} \tag{62}$$

$$C_D^i = \frac{C_D^{i-1}(1 - \frac{SY_{10}\Delta t}{2V_S}) + \frac{S(Y_4 - Y_7)\Delta t}{2V_S}(C_A^i + C_A^{i-1}) + \frac{S(Y_5 - Y_8)\Delta t}{2V_S}(C_B^i + C_B^{i-1})\frac{S(Y_6 - Y_9)\Delta t}{2V_S}(C_C^i + C_C^{i-1})}{1 + \frac{SY_{10}\Delta t}{2V_S}} \tag{63}$$

$$C_E^i = C_E^{i-1} + \frac{S\Delta t}{2V_S}[Y_7(C_A^{i-1} + C_A^i) + Y_8(C_B^{i-1} + C_B^i) + Y_9(C_C^{i-1} + C_C^i) + Y_{10}(C_D^{i-1} + C_D^i)] \tag{64}$$

$$C_F^i = \frac{C_F^{i-1}(1 - \frac{SY_{11}\Delta t}{2V_S}) + k_5(C_A^i + C_A^{i-1})\frac{\Delta t}{2}}{1 + \frac{SY_{11}\Delta t}{2V_S}} \quad (65)$$

$$C_G^i = \frac{C_G^{i-1}(1 - \frac{k_7\Delta t}{2}) + (C_F^i + C_F^{i-1})\frac{SY_{11}\Delta t}{2V_S}}{1 + \frac{k_7\Delta t}{2}} \quad (66)$$

The choice of Δt is 10 s for an electrolysis lasting several hours. The calculation results are invariant for time steps Δt below 20 s.

Appendix 3: Calculation of Rate Constants k_5 and k_7

The rate constant k_5 of chemical reaction (5), was determined from experimental data [21]. This reaction had a pseudo order of 1 with respect to **A** and with respect to sulphuric acid which catalyses the reaction. Thus, the rate of Reaction (5) is expressed as follows: $r_5 = k'_5[H_2SO_4][\mathbf{A}] = k_5[\mathbf{A}]$ where $k_5 = k'_5[H_2SO_4]$. The activation energy is 144.2 kJ mol^{-1}. Table 2 shows different values of k'_5.

The rate constant for Reaction (7) k_7 was obtained from the literature [25, 27]. The expression is: $k_7 = a + b\,[H_2SO_4]$, where a and b vary with the temperature in accordance with Arrhenius' law. The activation energy is 28.2 kJ mol^{-1}. The values of k_7 are shown in Table 2.

Appendix 4: Calculation of Mass Transfer Constants k_{dX}

The mass transfer constants were calculated for each electroreducible species according to the temperature and the acidity of the medium [28–31]. Carlsson's correlation [28] was used for the ELECTROCELL AB reactor with a turbulence promoter:

$$k_{dX} = 5.57(D_X/d_h)R_e^{0.4}S_c^{1/3} \quad (67)$$

The diffusion coefficients were calculated from the Wilke-Chang correlation [30]:

$$D_X = [1.173 \times 10^{-13}(2.6M_X)^{0.5}T]/(\mu V_{mX}^{0.6}) \quad (68)$$

The molar volumes V_{mX} (m^3 kmol^{-1}) were calculated taking into account the different atoms and functional groups [29]. The values used in the model were obtained as follows:

$$V_{mA} = 0.1743;\ V_{mF} = 0.1319;\ V_{mB} = 0.1153;$$
$$V_{mC} = 0.1227;\ V_{mD} = 0.1153$$

The values of mass transfer constants are shown in Table 3; μ is the viscosity of the sulphuric acid solution.

References

1. K. Scott, *Electrochim. Acta* **30** (1985) 245.
2. K. Scott, I.F. McConvey and A.N. Haines, *J. Appl. Electrochem.* **17** (1987) 925.
3. K. Scott, *J. Electroanal. Chem.* **248** (1988) 1.
4. I.F. McConvey, A.N. Haines and K. Scott, *Chem. Eng. Res. Des.* **67** (1989) 14.
5. K. Scott, *Electrochim. Acta* **38** (1993) 2155.
6. K. Scott, *Acta Chem. Hungarica* **130** (1993) 581.
7. K. Scott, *J. Appl. Electrochem.* **21** (1991) 945.
8. A.M. Romulus and A. Savall, *in* F. Lapicque, A. Storck and A.A. Wragg (Eds), 'Electrochemical Engineering and Energy', (Plenum Press, New York, 1994).
9. C. Amatore and J.M. Savéant, *J. Electroanal. Chem.* **123** (1981) 189.
10. K.M. Yin, T. Yeu and R.E. White, *J. Electrochem. Soc.* **138** (1991) 1051.
11. K. Scott, *Electrochim. Acta* **30** (1985) 235.
12. F. Fournier and M.A. Latifi, *J. Appl. Electrochem.* **28** (1998) 351.
13. T.V. Nguyen, C.W. Walton and R.E. White, *J. Electrochem. Soc.* **133** (1986) 1130.
14. D.H. Coleman and R.E. White, *J. Electrochem. Soc.* **142** (1995) 1152.
15. K. Scott, *J. Electroanal. Chem.* **243** (1988) 1.
16. G.P. Sakellaropoulos, *A.I.Ch.E. J.* **25** (1979) 781.
17. L. Weise, G. Valentin and A Storck, *J. Appl. Electrochem.* **16** (1986) 851.
18. A.M. Romulus and A. Savall, *J. Appl. Electrochem.* **30** (2000) 967.
19. A.M. Romulus and A. Savall, *J. Appl. Electrochem.* **29** (1999) 221.
20. A.M. Romulus, Université Paul Sabatier, Thèse (1993), Toulouse, France.
21. L. Eberson and J.H.P. Utley, *in* M. Baizer (Ed), 'Organic Electrochemistry', Chap 11, (M. Dekker Inc., New York, 1983).
22. M. Ferles and M. Prystas, *Collection Czechoslov. Chem. Commun.* **24** (1959) 3326.
23. W. Zheng-Hao and H. Zhi-Bin, *Electrochim. Acta* **30** (1985) 779.
24. R. Rodriguez-Amaro, R. Pérez, V. Lopez and J. Ruiz, *J. Electroanal. Chem.* **278** (1990) 307.
25. E. Laviron, Université de Dijon, Thèse (1961), Dijon, France.
26. V.N. Leibzon, A.P. Churilina, A.S. Mendkovich and V.P. Gultyai, *J. Electroanal. Chem.* **261** (1989) 165.
27. O.R. Brown, J.A. Harrison and K.S. Sastry, *J. Electroanal. Chem.* **58** (1975) 387.
28. L. Carlsson, B. Sandegren and D. Simonsson, *J. Electrochem. Soc.* **130** (1983) 342.
29. J.M. Coulson and J.F. Richardson, *Chemical Engineering* (Pergamon, Oxford, 1986).
30. C.R. Wilke and P. Chang, *A.I.Ch.E. J* **1** (1955) 264.
31. Handbook of Chemistry and Physics, (CRC Press, Boca Raton, 1987–1988).